Latin American Journal of Solids and Structures
www.lajss.org

Free Vibration Analysis of Functionally Graded Nanocomposite Beams on Elastic Foundation Using a Mesh-Free Method

Abstract

The use of Carbon Nanotubes as the reinforcing constituent for polymer matrix composites in place of conventional fibers has led to the emergence of a new generation of advanced composite materials. In this paper, the free vibration of functionally graded nanocomposite beams on elastic foundations are studied. Three different types of Carbon Nanotubes distributions in the polymer matrix material are studied; Uniform distribution, symmetrically functionally graded distribution and unsymmetrically functionally graded distribution. The analysis is carried out by a mesh-free method using the two-dimensional theory of elasticity. The Moving Least Square shape functions are implemented to approximate the displacement field. Due to the absence of the Kronecker delta property of the shape functions, a transformation technique is used to apply the essential boundary conditions. After validation, the effects of different design parameters such as Carbon Nanotubes distribution, slenderness ratios, boundary conditions and foundation stiffness on the vibrational behavior of the structure are investigated. It can be seen that from a design perspective, the vibrational response of a FG structure may be controlled in two ways; one way is through changing the distribution of the CNT's in the matrix material and the other way is by changing stiffness of the elastic foundation on which it is resting. A notable observation is that increasing the stiffness of the foundation will move the neutral axis away from the foundation support of the beam. The current approach can serve as a benchmark against which other semi-analytical and numerical methods based on classical beam theories can be compared.

Keywords

Functionally graded material, Carbon Nanotubes, Vibration, Mesh-free method, Elastic foundation.

Alireza Sayyidmousavi [a, *]
Mehrdad Foroutan [b]
Zouheir Fawaz [c]

[a] Ryerson University, Canada
asayyidmousavi@ryerson.ca
[b] Razi University, Iran
Foroutan@razi.ac.ir
[c] Ryerson University, Canada
Zfawaz@ryerson.ca

* Corresponding author

http://dx.doi.org/10.1590/1679-78253302

Received 12.08.2016
In revised form 08.08.2017
Accepted 08.08.2017
Available online 26.08.2017

1 INTRODUCTION

Carbon NanoTubes (CNT's), due to their supreme mechanical, thermal and electrical properties, have recently attracted numerous applications in different fields. [Dai (2007), Kang et al. (2006), Lau et al. (2006)] In particular, their use as the reinforcing constituent for polymer matrix composites in place of conventional fibers has led to the emergence of a new generation of advanced composite materials.

However, one problem with the application of CNT's as the reinforcing agent in polymers is the weak interfacial bonding between the CNT's and the matrix. This shortcoming can be alleviated through the use of Functionally Graded Materials (FGM's) in which material properties vary smoothly and continuously [Yas and Samadi (2012)]. This smooth variation of material properties is a major advantage of FGM's over conventional laminated composites where the sudden change in material properties across the interface causes delamination. In addition, in FGM's, the volume fractions of the constituents can be tailored for optimal performance of the structure [Qian and Ching (2011)]. It has been suggested by Shen (2009) that using the concept of FGM, i.e., gradual distribution of CNT's in the matrix material can considerably improve the interfacial bonding strength between the CNT's and the matrix.

Although a large amount of research has been dedicated to accurately obtaining the mechanical properties of Carbon NanoTube-Reinforced Composites (CNTRC's) [Odegard et al. (2003), Hu et al. (2005), Fidelus et al. (2005), Bonnet et al. (2007), Han and Elliot (2007), Zhu et al. (2007)], not as many studies have yet been conducted on the global response of CNTRC's to actual structural loading conditions in practical applications which is of course the ultimate purpose for the design and development of such materials.

One example of practical applications of such advanced composite materials are in structures resting on elastic foundations. In particular, FGM beams on elastic foundations are often used to describe a lot of engineering problems and has application in geotechnics, road, railroad and marine engineering and bio-mechanics. The selection of the proper CNT's distribution and foundation stiffness are two important aspects to be taken into account in the design of such structures

In the literature, the works on FGM beams resting on elastic foundations can be classified into two main categories. The first group used analytical and semi-analytical methods to study the bending and vibrations of FG beams resting on elastic foundations. Ying et al. (2008) presented exact solutions for functionally graded simply supported beams resting on a Winkler–Pasternak elastic foundation based on the two-dimensional theory of elasticity. Fallah and Aghdam (2011) studied the free vibration and post-buckling of FG beams on nonlinear elastic foundations subject to axial loads. They used He's variational method to get the approximate closed form solution of the nonlinear governing equation. Arefi (2014) studied the nonlinear response of FG beams on elastic foundations and spring supports using Adomians Decomposition and successive approximation methods for the solution of the nonlinear differential equation. Yaghoobi and Torabi (2013) used the Variational Iteration Method to study the post-buckling and vibration of geometrically imperfect FG beams resting on elastic foundation. The Variational Iteration Method was also used by Kanani et al. (2014) to study the free and forced vibrations of FG beams on elastic foundations. The second group of works utilized numerical methods to investigate static and dynamic behavior of FGM beams resting on elastic foundations. From among numerical methods, the Finite Element

Method (FEM) has widely been used for this purpose. Examples of research studies using the FE method are the works done by Abbas and Thomas (1978), Ozturk and Sabuncu (2005), Mohanty et al. (2011). Differential quadrature (DQ) method is another numerical scheme used to study the bending and vibration of FGM beams on elastic foundations. Researchers who have used the DQ method to this aim include Pradhan and Murmu (2009); Esfahani et al. (2013); Yas and Samadi (2012).

In recent years, mesh free methods have been used as an efficient numerical method to solve different initial-boundary-value problems. Unlike the finite element method (FEM), in mesh-free methods the physical problem domain is modeled by only a set of scattered nodes without the need to be connected to form a closed polygon. The main advantage of mesh-free methods as compared to the FEM is the elimination of the mesh generation phase which can therefore save a considerable amount of time in the pre-processing phase. In addition, the computed stress by Mesh free methods result in smooth strain and stress fields without the need for any post-processing technique. As for functionally graded materials, since in mesh-free methods unlike the FEM, the material variation is captured at the integration points, fewer nodes will be required in the analysis of the problem for the same level of accuracy [Qian and Ching (2011)]. Different mesh-free methods have so far been proposed. Examples are the Diffuse Element Method (DEM) [Nayroles et al. (1992)], the Element-Free Galerkin (EFG) method [Belytschko et al. (1994)], the Hp-Clouds method [Duarte and Oden (1996)], the Reproducing Kernel Particle Method (RKPM) [Liu et al. (1995)], the Partition of Unity Finite Element Method (PUFEM) [Melenk and Babuska (1996)], and the Meshless Local Petrov-Galerkin (MLPG) method. [Alturi and Zhu (2000)]

One of the most frequently used mesh-free methods in the analysis of solid mechanic problems is the Element Free Galerkin (EFG) method which utilizes the moving least square (MLS) shape functions. The main challenge in this method is the imposition of the essential boundary conditions due to the absence of the Kronecker delta property of the MLS shape function. To overcome this problem, the EFG method utilizes the Lagrange Multipliers Scheme for the imposition of the essential boundary conditions. However, this will be at the cost of increasing the number of degrees of freedom and resulting in a non-positive definite system matrix. In order to circumvent the afore-mentioned issue, in the present paper, the transformation technique [Moradi-Datjerdi et al. (2013)] is used to impose the essential boundary conditions. In this technique, after the correction of the mesh-free shape functions, the essential boundary conditions are imposed as in the FEM causing the number of the degrees of freedom to remain unchanged. A very recent work using MLS shape functions is the study of the free vibration of functionally graded cylindrical panels in 3 dimensions conducted by Soltanimaleki et al. (2015). The bulk of the works in the literature are based on the assumptions of beam theories; mostly Euler-Bernoulli and Timoshenko. However, beam is a three-dimensional structure and although Timoshenko theory is an improvement on the Euler Bernoulli theory, the assumptions of the beam theories may not accurately represent the actual response of the structure [Labuschagne et al. (2009)]. The objective of the present work is to study the vibration of functionally graded nanocomposite beams resting on Winkler and Pasternak foundation using the two-dimensional theory of elasticity by a mesh-free method. In addition to the practical applications of the problem under consideration, the distinctive features of the current work are the use of a meshless method considering the afore-mentioned advantages and the two dimensional elas-

ticity solution which can give a more realistic representation of the structure compared to beam theories especially as the aspect ratio of the beam increases.

The FG beam in this study is reinforced by randomly oriented Single-Walled Carbon Nano-Tubes (SWCNT's). It is assumed that the material properties vary in the thickness direction and are approximated using the Mori-Tanaka method [Mori and Tanaka (1973)]. In the mesh-free method, the moving least square (MLS) shape functions are implemented to approximate the displacement field. The model is validated through comparison with the exact solution both for thick and thin beams. Once validated, the effects of different design parameters such as CNT's distribution, slenderness ratios, boundary conditions and foundation stiffness on the vibrational behavior of the structure are investigated.

2 MATERIAL PROPERTIES

As the reinforcing constituent, CNT's are either aligned or randomly oriented in the isotropic matrix material. The effects of randomly oriented CNT's on the elastic properties of CNTRC's have been thoroughly investigated by Shi et al. (2004). Figure 1 shows a representative volume element of a polymer matrix reinforced with randomly oriented straight CNT's. The orientation of the straight CNT is identified by angles α and β.

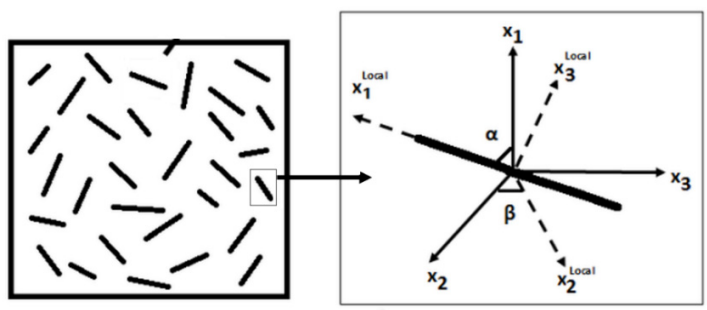

Figure 1: Representative volume element of a polymer matrix reinforced with randomly oriented straight CNT's.

According to shi et al. (2004), despite the CNT's having transversely isotropic properties, when the CNT's are randomly oriented in the matrix, the composite material can be modeled as an isotropic material. The effective properties of the isotropic materials is derived using the Mori-Tanaka approach. The Mori-Tanaka method is based on the assumption that each inclusion is embedded in the pristine matrix and subjected to far field average stress and strain [Mori and Tanaka (1973)]. The effective bulk modulus K and shear modulus G are defined as [Shi et al. (2004)]:

$$K = K_m + \frac{V_r(\delta_r - 3K_m\alpha_r)}{3(V_m + V_r\alpha_r)} \tag{1}$$

$$G = G_m + \frac{f_r(\eta_r - 2G_m\beta_r)}{3(V_m + V_r\beta_r)} \tag{2}$$

where K_m and G_m are the shear and bulk moduli of the matrix material, respectively. V_r and V_m denote the volume fractions of reinforcements and matrix, respectively and

$$\alpha_r = \frac{3(K_m + G_m) + k_r - l_r}{3(G_m + k_r)} \tag{3}$$

$$\beta_r = \frac{1}{5}\left\{\frac{4G_m + 2k_r + l_r}{3(G_m + k_r)} + \frac{4G_m}{G_m + p_r} + \frac{2\left[G_m(3k_m + G_m) + G_m(3K_m + 7G_m\right]}{G_m(3K_m + G_m) + m_r(3K_m + 7G_m)}\right\} \tag{4}$$

$$\delta_r = \frac{1}{3}\left\{n_r + 2l_r + \frac{(2k_r + l_r)(3K_m + G_m - l_r)}{G_m + k_r}\right\} \tag{5}$$

$$\eta_r = \frac{1}{5}\left\{\frac{2}{3}(n_r - l_r) + \frac{8G_m p_r}{G_m + p_r} + \frac{8m_r G_m(3K_m + 4G_m)}{3K_m(m_r + G_m) + G_m(7m_r + G_m)} + \frac{2(k_r - l_r)(2G_m + l_r)}{3(G_m + k_r)}\right\} \tag{6}$$

k_r, l_r , m_r , n_r and p_r are the Hill's elastic moduli of the CNT's. The effective Young's Modulus E and Poisson's ratio υ are defined as:

$$E = \frac{9KG}{3K + G} \tag{7}$$

$$\upsilon = \frac{3K - 2G}{6K + 2G} \tag{8}$$

The volume fractions of the reinforcement V_r and matrix V_m are related as:

$$V_r + V_m = 1 \tag{9}$$

Three different cases are investigated; uniform distribution (UD), symmetrically functionally graded (SFG) distribution and unsymmetrically functionally graded (USFG) distribution. The reinforcement volume fraction V_r for each case is defined as follows:

$$V_r = \widehat{V}_r \qquad UD \tag{10}$$

$$V_r = \frac{4|y|}{h}\widehat{V}_r \qquad SFG \tag{11}$$

$$V_r = (1 - \frac{2y}{h})\widehat{V}_r \qquad USFG \tag{12}$$

Where

$$\widehat{V}_r = \frac{w_r}{w_r + (\frac{\rho_r}{\rho_m}) - (\frac{\rho_r}{\rho_m})w_r} \tag{13}$$

w_r is the mass fraction of reinforcement. ϱ_r and ϱ_m are the densities of reinforcement and matrix, respectively. The mass density of the composite is calculated using the rule of mixtures:

$$\rho = \rho_r V_r + \rho_m V_m \tag{14}$$

Carbon Nanotubes are distributed in the matrix material in three different patterns; uniformly distributed, resulting in a uniform volume fraction through the thickness; symmetrically distributed in which the volume fraction of the reinforcement is minimum on the neutral axis and linearly increases away from the neutral axis in the y direction and the unsymmetric distribution in which the volume fraction linearly increases through the thickness from the top to the bottom. Figure 2 schematically shows the FG beam cross sections for the three different CNT's distribution types. Table 1 lists the material properties of the SWCNT's reinforcement predicted through replacement with an equivalent long fiber [Yas and Heshmati (2012)].

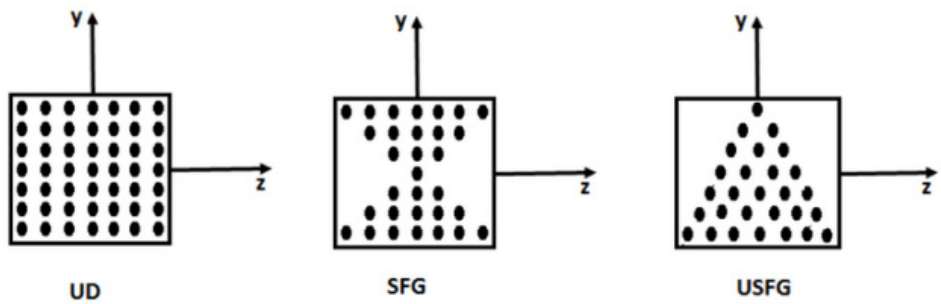

Figure 2: Schematic representation of the CNT's distribution within the matrix material.

Material Property	
Longitudinal Modulus	649.12 (GPa)
Transverse Modulus	11.27 (GPa)
Longitudinal Shear Modulus	5.13 (GPa)
Poisson's ratio	0.284
Density	1400 (kg/m3)

Table 1: Material properties of the SWCNT's reinforcement [Yas and Heshmati, (2012)].

3 PROBLEM FORMULATION

The standard variational form of the equation of motion is expressed as follows:

$$\int_{\Omega} (\delta\boldsymbol{\varepsilon})^T \boldsymbol{\sigma}.d\Omega - \int_{\Gamma} (\delta\mathbf{u})^T \mathbf{F} d\Gamma = -\int_{\Omega} (\delta\mathbf{u})^T \rho\ddot{\mathbf{u}} d\Omega \tag{15}$$

where $\boldsymbol{\sigma}$, $\boldsymbol{\varepsilon}$, $\mathbf{F}$, $\mathbf{u}$ and $\ddot{\mathbf{u}}$ represent stress, strain, surface traction, displacement and acceleration vectors respectively. Γ is a part of boundary of domain Ω on which traction $\mathbf{F}$ is applied. Stress and strain vectors are related through Hook's law:

$$\boldsymbol{\sigma} = \mathbf{D}\boldsymbol{\varepsilon} \tag{16}$$

In the present work, moving least square (MLS) shape functions introduced by Lancaster and Salkauskas (1981) are used to approximate the displacement vector $\mathbf{u}$ at any point of interest using the nodes in the local support domain of that point. For a two dimensional problem:

$$\mathbf{u} = \boldsymbol{\varphi}\hat{\mathbf{u}} \tag{17}$$

$\boldsymbol{\Phi}$ and $\hat{\mathbf{u}}$ are the shape function matrix and the nodal values vector, respectively; n denotes the number of the nodes in the local support domain of the point of interest.

$$\boldsymbol{\varphi} = \begin{bmatrix} \phi_1 & 0 & \dots & \phi_n & 0 \\ 0 & \phi_1 & \dots & 0 & \phi_n \end{bmatrix} \tag{18}$$

$$\hat{\mathbf{u}} = \begin{bmatrix} u_1 & v_1 & \dots & u_n & v_n \end{bmatrix}^T \tag{19}$$

The strain-displacement relation can be expressed in terms of the nodal values $\hat{\mathbf{u}}$ as follows:

$$\boldsymbol{\varepsilon} = \mathbf{B}\hat{\mathbf{u}} \tag{20}$$

where

$$\mathbf{B} = \begin{bmatrix} \frac{\partial \phi_1}{\partial x} & 0 & \dots & \frac{\partial \phi_n}{\partial x} & 0 \\ 0 & \frac{\partial \phi_1}{\partial y} & \dots & 0 & \frac{\partial \phi_n}{\partial y} \\ \frac{\partial \phi_1}{\partial y} & \frac{\partial \phi_1}{\partial x} & \dots & \frac{\partial \phi_n}{\partial y} & \frac{\partial \phi_n}{\partial x} \end{bmatrix} \tag{21}$$

Substituting equations 16, 17 and 20 into the equation of motion yields:

$$\delta(\hat{\mathbf{u}})^T \left(\int_\Omega \mathbf{B}^T \mathbf{D}\mathbf{B} d\Omega\right)\hat{\mathbf{u}} - \delta(\hat{\mathbf{u}})^T \int_\Gamma \boldsymbol{\varphi}^T \mathbf{F} d\Gamma = -\delta(\hat{\mathbf{u}})^T \left(\int_\Omega \rho \boldsymbol{\varphi}^T \boldsymbol{\varphi} d\Omega\right)\ddot{\hat{\mathbf{u}}} \tag{22}$$

In the above-given equation the surface traction will be the reaction force of the elastic foundation which can be written in terms of nodal displacements:

$$\mathbf{F} = \mathbf{K}_\mathbf{W}\boldsymbol{\varphi}\hat{\mathbf{u}} + \mathbf{K}_\mathbf{P}\frac{\partial^2 \boldsymbol{\varphi}}{\partial x^2}\hat{\mathbf{u}} \tag{23}$$

where $\mathbf{K_W}$ and $\mathbf{K_P}$ are defined as follows:

$$\mathbf{K}_\mathbf{W} = \begin{bmatrix} 0 & 0 \\ 0 & -k_w \end{bmatrix} \tag{24}$$

$$\mathbf{K_P} = \begin{bmatrix} 0 & 0 \\ 0 & k_p \end{bmatrix} \tag{25}$$

$\mathbf{K_W}$, known as the Winkler coefficient, is the spring stiffness of the foundation controlling the transverse deflection of the structure. $\mathbf{K_P}$, known as Pasternak coefficient, is the stiffness of a shear layer which accounts for the shear interactions on the vertical springs of the foundation. Figure 3 shows the geometry of a beam on Winkler-Pasternak foundation.

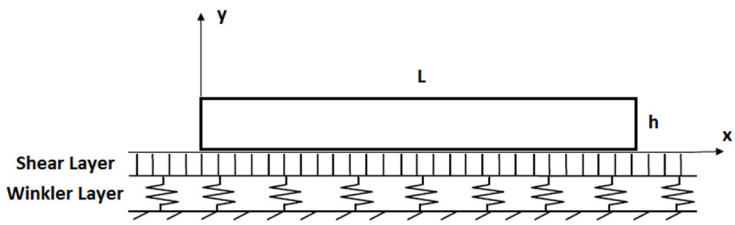

Figure 3: The geometry of the beam on a Winkler-Pasternak foundation.

Rearranging equation 22 considering the fact that it should hold for any arbitrary $\delta(\hat{\mathbf{u}})^{\mathrm{T}}$ leads to :

$$\mathbf{M}\ddot{\hat{\mathbf{U}}} + \mathbf{K}\hat{\mathbf{U}} = \mathbf{0} \tag{26}$$

where

$$\hat{\mathbf{U}} = \begin{bmatrix} u_1 & v_1 & \dots & u_N & v_N \end{bmatrix}^T \tag{27}$$

$$\mathbf{K} = \int_{\Omega} \mathbf{B}^T \mathbf{D}\mathbf{B} d\Omega - \int_{\Gamma} \boldsymbol{\varphi}^{\mathbf{T}} \mathbf{K}_{\mathbf{W}} \boldsymbol{\varphi} d\Gamma - \int_{\Gamma} \boldsymbol{\varphi}^{\mathbf{T}} \mathbf{K}_{\mathbf{P}} \frac{\partial^2 \boldsymbol{\varphi}}{\partial x^2} d\Gamma \tag{28}$$

$$\mathbf{M} = \int_{\Omega} \rho \boldsymbol{\varphi}^T \boldsymbol{\varphi} d\Omega \tag{29}$$

N is the total number of nodes in the problem domain. For numerical integration, the problem domain is discretized to a set of background cells with gauss points inside each cell. Then global stiffness matrix $\mathbf{K}$ is obtained numerically by sweeping all gauss points inside Ω. . Similarly global force vector $\mathbf{f}$ is formed numerically in the same manner but by sweeping all gauss points on Γ. Since the MLS shape functions do not possess the Kronecker delta property, the essential boundary conditions may not be directly imposed on the nodal vector $\hat{\mathbf{U}}$. To alleviate this problem, a transformation matrix is constructed which relates the real nodal displacement vector, $\mathbf{U}$ to $\hat{\mathbf{U}}$:

$$\mathbf{U} = \mathbf{T}\hat{\mathbf{U}} \tag{30}$$

where

$$\mathbf{T}=\begin{bmatrix} \phi_1(X_1) & 0 & \phi_2(X_1) & 0 & ... & \phi_N(X_1) & 0 \\ 0 & \phi_1(X_1) & 0 & \phi_2(X_1) & ... & 0 & \phi_N(X_1) \\ \vdots & \vdots & \vdots & \vdots & \vdots & \vdots & \vdots \\ \phi_1(X_N) & 0 & \phi_2(X_N) & 0 & ... & \phi_N(X_N) & 0 \\ 0 & \phi_1(X_N) & 0 & \phi_2(X_N) & ... & 0 & \phi_N(X_N) \end{bmatrix} \tag{31}$$

Using equation 30, equation 26 can be rewritten as:

$$\hat{\mathbf{M}}\ddot{\mathbf{U}}+\hat{\mathbf{K}}\mathbf{U}=\mathbf{0} \tag{32}$$

where

$$\hat{\mathbf{M}}=\mathbf{T}^{-T}\mathbf{M}\mathbf{T}^{-1} \qquad \hat{\mathbf{K}}=\mathbf{T}^{-T}\mathbf{K}\mathbf{T}^{-1} \tag{33}$$

The essential boundary conditions can now be imposed on the modified system (equation 32) similar to the finite element analysis.

4 RESULTS

Table 2 lists the fundamental frequency parameters for simply supported beams on Winkler and Pasternak foundations compared with the exact solution obtained by Chen et al. (2004). They assumed trigonometric functions for the variations of the axial deflection, transverse deflection, transverse normal stress and shear stress such that simply supported end conditions are satisfied. The results are seen to be in very good agreement with the literature for both thin and thick beams.

Foundation Stiffness		L/h=120		L/h=15		L/h=5	
$\bar{k}_w$	$\bar{k}_p/\pi 2$	Present	Exact [Chen et al. (2004)]	Present	Exact [Chen et al. (2004)]	Present	Exact[Chen et al. (2004)]
0	0	3.142080	3.141417	3.130338	3.1302475	3.048003	3.0479950
	0.5	3.478399	3.476589	3.468103	3.4667123	3.395937	3.3945841
	1.0	3.738382	3.735859	3.728751	3.7265663	3.660169	3.6580220
	2.5	4.300635	4.296879	4.291623	4.2880929	4.221790	4.2183417
100	0	3.748612	3.748219	3.739004	3.7389477	3.670508	3.6705003
	0.5	3.961896	3.960669	3.952622	3.9516807	3.884874	3.8839762
	1.0	4.145417	4.143565	4.136320	4.1347188	4.067915	4.0663637
	2.5	4.585363	4.582264	4.576383	4.5734720	4.501957	4.4991384
10000	0	10.024074	10.02404	9.995839	9.9958219	7.340804	7.3408115
	0.5	10.036194	10.03610	10.007854	10.007782	7.340877	7.3408839
	1.0	10.048271	10.04813	10.019825	10.019699	7.340948	7.3409553
	2.5	10.084243	10.08394	10.055478	10.055193	7.341157	7.3411636

Table 2: Fundamental frequency parameters for simply supported beams on Winkler and Pasternak foundations.

The convergence process of the above-obtained results is highlighted in table 3 showing how the dimensionless natural frequency of the beam vary with the number of nodes. The convergence is seen to have occurred for *N=91x19* which will be used for the analyses and modified accordingly for different slenderness ratios.

Foundation Stiffness		Number of nodes				
$\bar{k}_W$	$\bar{k}_P/\pi 2$	21X5	31X7	61X13	91X19	121X25
100	0	3.670611	3.670551	3.670515	3.670508	3.670505
	0.5	3.884931	3.884900	3.884879	3.884874	3.884872
	1.0	4.067940	4.067929	4.067918	4.067915	4.067914
	2.5	4.501920	4.501947	4.501956	4.501957	4.501957

Table 3: Variations of the fundamental frequency parameter with the number of nodes (L/h=5).

Table 4 shows how the first 3 dimensionless frequencies for different distribution types and volume fractions vary with foundation stiffness. The introduction of Winkler and Pasternak foundations are seen to increase the rigidity and consequently the frequency parameter of the structure. The frequencies and stiffness foundations are nondimensionalized as follows:

$$\varpi = \omega L\sqrt{\frac{I_1}{A_{11}}} \qquad \bar{k}_W = \frac{K_W L^2}{A_{11}} \qquad \bar{k}_P = \frac{K_P}{A_{11}} \tag{34}$$

A_{11} and I_{11} are the stiffness and inertia terms of a homogeneous beam.

$\hat{V}_r$		$(\bar{k}_W,\bar{k}_P)=(0,0)$			$(\bar{k}_W,\bar{k}_P)=(0.1,0)$			$(\bar{k}_W,\bar{k}_P)=(0.1,0.05)$		
		$\bar{\omega}1$	$\bar{\omega}2$	$\bar{\omega}3$	$\bar{\omega}1$	$\bar{\omega}2$	$\bar{\omega}3$	$\bar{\omega}1$	$\bar{\omega}2$	$\bar{\omega}3$
0.11	UD	1.1299	2.6864	3.8633	1.1712	2.7032	3.8634	1.3750	3.0236	3.8668
	SFG	1.1762	2.7274	3.8485	1.2160	2.7441	3.8486	1.4119	3.0618	3.8519
	USFG	1.1023	2.6311	3.8479	1.1447	2.6484	3.8479	1.3546	2.9794	3.8505
0.16	UD	1.2174	2.8935	4.1645	1.2554	2.9089	4.1646	1.4458	3.2064	4.1678
	SFG	1.2693	2.9259	4.1389	1.3059	2.9413	4.1390	1.4882	3.2377	4.1422
	USFG	1.1730	2.8046	4.1376	1.2125	2.8206	4.1376	1.4112	3.1313	4.1402
0.26	UD	1.3619	3.2346	4.6641	1.3953	3.2481	4.6642	1.5658	3.5121	4.6673
	SFG	1.4152	3.2369	4.6146	1.4475	3.2506	4.6147	1.6106	3.5166	4.6177
	USFG	1.2865	3.0833	4.6122	1.3219	3.0975	4.6122	1.5035	3.3781	4.6148

Table 4: The first 3 dimensionless frequencies ($\bar{\omega}$) for different distribution types and volume fractions (L/h=5).

Figure 4 shows the variations dimensionless fundamental frequency for different CNT's distribution types against the stiffness of the Winkler layer. It can be seen that for a given CNT's volume fraction and foundation stiffness, due to the symmetrically linear distribution of CNT's in the matrix material i.e., the existence of more CNT's in the high bending stress regions farther from the neutral axis, the SFG has the highest bending stiffness and consequently the highest natural frequency of all the three cases. Similarly, the unsymmetrical distribution of CNT's leads to the USFG distribution type having the lowest natural frequency.

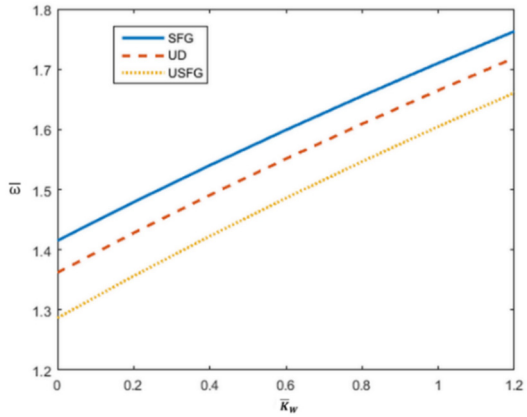

Figure 4: Effect of the stiffness of the Winkler springs on dimensionless fundamental frequency (C-C) $\widehat{\boldsymbol{V}}_{\boldsymbol{r}} = \mathbf{0.26}$, L/h=5, $\bar{\boldsymbol{k}}\boldsymbol{p} = \mathbf{0}$.

In figure 5, the effect of the shear layer stiffness on the fundamental frequency of the structure is illustrated for two different slenderness ratios. Increasing the foundation stiffness results in a more rigid structure thereby giving rise to the frequency of the vibration. From a design perspective, the vibrational response of a FG structure may be controlled in two ways; one way is through changing the distribution of the CNT's in the matrix material and the other way is by changing stiffness of the elastic foundation on which it is resting. However, as can be seen for thin beams, the latter approach seems more practical.

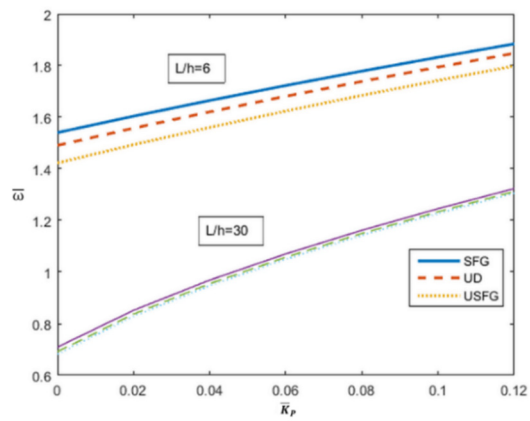

Figure 5: Effect of the shear layer stiffness on dimensionless fundamental frequency (C-C) $\widehat{\boldsymbol{V}}_{\boldsymbol{r}} = \mathbf{0.26}$, L/h=5, $\bar{\boldsymbol{k}}\boldsymbol{w} = \mathbf{0.4}$.

How Winkler foundation stiffness affects the fundamental frequency of the structure is depicted in figure 6. It is observed that increasing Winkler stiffness increases the frequency of the vibration; however, the rate of this increase gradually diminishes such that after a certain value of stiffness, no sensible change in the frequency occurs.

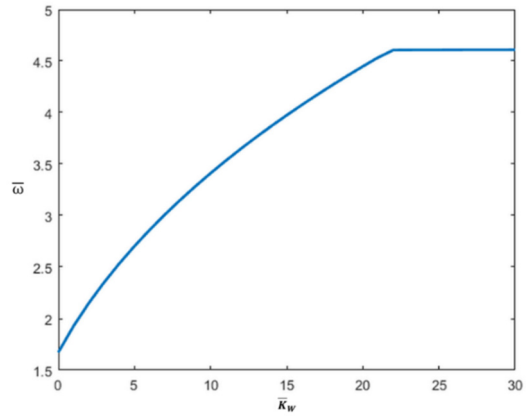

Figure 6: Variations of dimensionless fundamental frequency with the stiffness of the Winkler springs (C-C) $\widehat{\boldsymbol{V}}_{\boldsymbol{r}} = \mathbf{0.26}$, L/h=5, $\overline{\boldsymbol{kp}} = \mathbf{0.08}$.

The variation of deformation along the thickness which may not be accurately described by simplified beam theories, can be investigated through the use of the dimensional elasticity. The use of two-dimensional elasticity theory as compared to beam theories will permit the investigation of through-thickness variations of deformations. The effect of elastic foundations on the through-thickness variations of the transverse deflections is presented in figure 7. A notable observation is that increasing the stiffness of the foundation will move the neutral axis away from the foundation support of the beam.

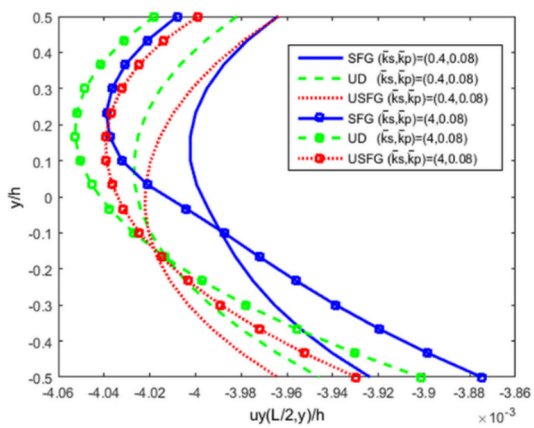

Figure 7: Through-thickness variations of the transverse deflections (C-C) $\widehat{\boldsymbol{V}}_{\boldsymbol{r}} = \mathbf{0.26}$, L/h=5.

The effect of CNT's volume fraction on the frequency of UD and SFG distribution is shown in figure 8. Increasing the volume fraction of the reinforcement is seen to increase the rigidity and consequently the natural frequency of the structure for both distribution types. While for low CNT's volume fraction, there is little difference between the responses of the SFG and UD beams, increasing the volume fraction of the reinforcement is seen to be highlighting the symmetrical distribution effect of the SFG beam on increasing the frequency parameter of the structure.

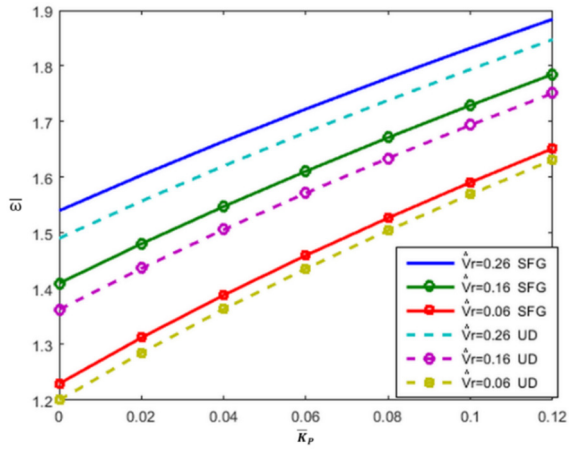

Figure 8: Effect of the CNT's volume fraction on dimensionless fundamental frequency (C-C) $\widehat{\boldsymbol{V}}_{\boldsymbol{r}} = \mathbf{0.26}$, L/h=5, $\bar{\boldsymbol{k}}\boldsymbol{w} = \mathbf{0.4}$.

To study the effect of boundary conditions on the vibration of the SFG beams four combinations of free, simply supported, and clamped boundaries designated as C-C, C-S, S-S, C-F have been considered as shown in Figure 9a. The letters F, S, and C denote free, simply supported and clamped, respectively. It is seen that the fundamental frequency increases with greater geometric constraint in the following sequence (C-F, C-S, S-S, and C-C) which is due to the increase in the bending stiffness of the structure. A noteworthy observation is that unlike other boundary conditions, for the C-F type, the fundamental frequency tends to slightly decrease with increasing the Pasternak stiffness. Such a trend, however, as seen in figure 9b, is not observed when increasing the Winkler stiffness of the structure.

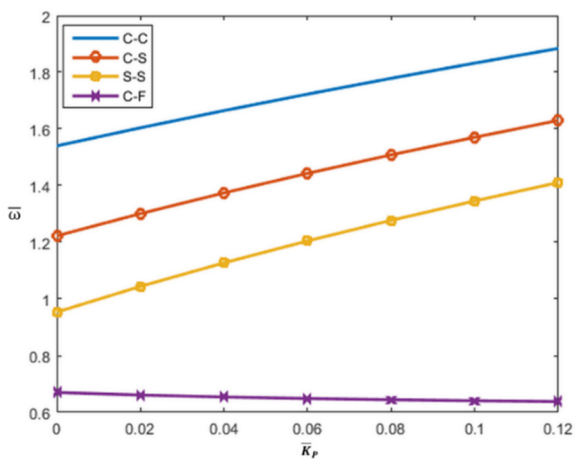

Figure 9a: Effect of boundary conditions on dimensionless fundamental frequency $\widehat{\boldsymbol{V}}_{\boldsymbol{r}} = \mathbf{0.26}$, L/h=5, $\bar{\boldsymbol{k}}\boldsymbol{w} = \mathbf{0.4}$.

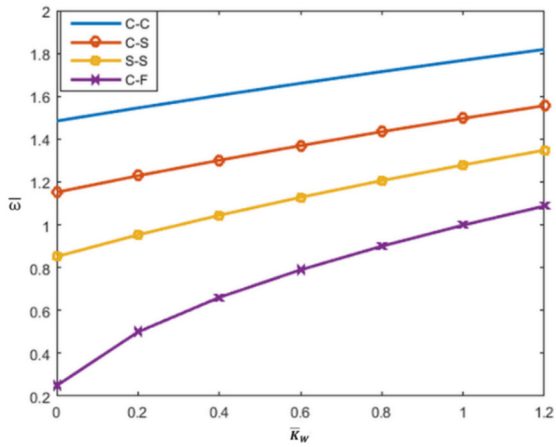

Figure 9b: Effect of boundary conditions on dimensionless fundamental frequency $\widehat{V}_r = 0.26$, L/h=5, $\bar{k}p = 0.02$.

5 CONCLUSIONS

The vibration behavior of functionally graded beams reinforced by randomly oriented SWCNT's on elastic foundations is studied using a mesh-free method. Three different types of CNT's distributions in the polymer matrix material are investigated; uniform distribution (UD), symmetrically functionally graded (SFG) distribution and unsymmetrically functionally graded (USFG) distribution. The current two dimensional elasticity approach can serve as a benchmark against which other semi-analytical and numerical methods based on classical beam theories can be compared. Based on the obtained results the following observations are made:

It is observed that for a given foundation stiffness, functionally graded CNT's with SFG i.e. the symmetric distribution has better capability to increase the frequency of the structure in comparison with other distribution types. This is because of the existence of more CNT's in the high bending stress regions farther from the neutral axis. In fact, the frequency of the structure can be controlled either by the distribution type of the CNT's in the matrix material or changing the stiffness of the elastic foundation. The rate of frequency increase due to foundation stiffness is seen to be higher for thin beams in comparison with thick beams. The results also indicate that increasing the stiffness of the foundation after a certain value has no impact on the frequency of the structure. Unlike beam theories, the present approach will allow one to investigate the deformation along the thickness direction. The results show that increasing the foundation stiffness moves the neutral axis away from the foundation support of the beam. Greater geometric constraint is seen to increase the flexural rigidity and thus the fundamental frequency of the structure. From the four different boundary conditions studied; C-F, C-S, S-S, and C-C, only for the C-F boundary condition, increasing the Pasternak stiffness of the foundation results in a slight decrease in the frequency of the beam.

Acknowledgement

This work was supported by the Natural Sciences and Engineering Research Council of Canada-Discovery Grant Program

References

Abbas, B.A.H., Thomas, J. (1978). Dynamic stability of Timoshenko beams resting on an elastic foundation. Journal of Sound and Vibration 60 (1): 33–44.

Arefi, M. (2014). Nonlinear analysis of a functionally graded beam resting on the elastic nonlinear foundation. Journal of Theoretical and Applied Mechanics 44: 71-82.

Atluri, S.N., Zhu, T. (2000). The Meshless Local Petrov-Galerkin (MLPG) Approach for solving problems in elasto-statics. Computational Mechanics 25(2): 169-179.

Belytschko, T., Lu, Y.Y., Gu, L. (1994). Element-Free Galerkin Methods. International Journal for Numerical Methods in Engineering 37(2): 229-256.

Bonnet, P., Sireude, D., Garnier, B., Chauvet, O. (2007). Thermal properties and percolation in carbon nanotube–polymer composites. Journal of Applied Physics 91, 2019–2030.

Chen, W.Q., Lu, C.F., Bian, Z.G. (2004). A mixed method for bending and free vibration of beams resting on a Pasternak elastic foundation. Applied Mathematical Modeling 28(10): 877-890.

Dai, H. (2007). Carbon nanotubes: Opportunities and challenges. Surface Science 500(1-3): 218–241.

Duarte, C.A., Oden, J.T. (1996). H-p Clouds — an hp Meshless Method. Numerical Methods for Partial Differential Equations. 12(1-4): 673-705.

Esfahani, S.E., Kiani, Y., Eslami, M.R. (2013). Non-linear thermal stability analysis of temperature dependent FGM beams supported on non-linear hardening elastic foundations. International Journal of Mechanical Sciences 69:10-20.

Fallah, A., Aghdam, M.M. (2011). Nonlinear free vibration and post-buckling analysis of functionally graded beams on nonlinear elastic foundation. European Journal of Mechanics, A/Solids 30:571-583.

Fidelus, J.D., Wiesel, E., Gojny, F.H., Schulte, K., Wagner, H.D. (2005). Thermo-mechanical properties of randomly oriented carbon/epoxy nanocomposites. Composites Part A. 36(11): 1555–1561.

Han, Y., Elliott, J. (2007). Molecular dynamics simulations of the elastic properties of polymer/carbon nanotube composites. Computational Materials Science 39, 315–323.

Hu, N., Fukunaga, H., Lu, C., Kameyama, M., Yan, B. (2005). Prediction of elastic properties of carbon nanotube reinforced composites. Proceedings A of the Royal Society 461, 1685–1910.

Kanani, A.S., Niknam, H., Ohadi, A.R., Aghdam, M.M. (2014). Effect of nonlinear elastic foundation on large amplitude free and forced vibration of functionally graded beam. Composite Structures 115: 60-68.

Kang, I., Heung, Y., Kim, J., Lee, J., Gollapudi, R., Subramaniam, S., Narasimhadevara, S., Hurd, D., Kirkera, G., Shanov, V., Schulz, M., Shi, D., Boerio, J., Mall, S., Ruggles-Wren, D. (2006). Introduction to carbon nanotube and nanofiber smart materials. Composites Part B. 37(6): 382–394.

Labuschagne, A., VanRensburg, N.F.J., Van der Merwe, A.J. (2009). Comparison of linear beam theories. Mathematical and Computer Modeling 49(1-2): 20-30.

Lancaster, P., Salkauskas, K. (1981). Surface generated by moving least squares methods. Mathematics of Computation 37(154): 141–58.

Lau, K.T., Gu, C., Hui, D. (2006). A critical review on nanotube and nanotube/nanoclay related polymer composite materials. Composites Part B. 37(6): 425–436.

Liu, W.K., Jun, S., Zhang, Y.F. (1995). Reproducing Kernel Particle Methods. International Journal for Numerical Methods in Engineering 38(10): 1081-1106.

Melenk, J.M., Babuska, I. (1996). The partition of Unity Finite Element Method: Basic theory and applications. Computer Methods in Applied Mechanics and Engineering 139(1-4): 289-314.

Mohanty, S.C., Dash, R.R., Rout, T. (2011). Parametric instability of a functionally graded Timoshenko beam on Winkler's elastic foundation Nuclear Engineering and Design 241: 2698-2715

Moradi-Dastjerdi, R. Foroutan, M., Pourasghar, A., (2013). Dynamic analysis of functionally graded nanocomposite cylinders reinforced by carbon nanotube by a mesh-free method. . Materials and Design 44, 256-266.

Mori, T., Tanaka, K. (1973). Average stress in matrix and average elastic energy of materials with misfitting inclusions Acta Metallurgica 21(5): 571–574.

Nayroles, B., Touzot, G., Villon, P. (1992). Generalizing the finite element method: Diffuse approximation and diffuse elements. Computational Mechanics 10(5): 307-318.

Odegard, G.M., Gates, T.S., Wise, K.E., Park, C., Siochi, E.J. (2003). Constitutive modeling of nanotube-reinforced polymer composites. Composite Science and Technology 63(11): 1671–1687.

Ozturk, H., Sabuncu, M. (2005). Stability analysis of a cantilever composite beam on elastic support. Composite Science and Technology 65: 1982–1995.

Pradhan, S.C., Murmu, T. (2009) Thermo-mechanical vibration of FGM sandwich beam under variable elastic foundations using differential quadrature method. Journal of Sound and Vibration 321:342-362.

Qian, L.F., Ching, H.K. (2011). Static and dynamic analysis of 2-D functionally graded elasticity by using meshless local petrov- galerkin method. Journal of Chinese Institute of Engineers 27(4): 491-503.

Shen, H.S. (2009). Nonlinear bending of functionally graded carbon nanotube reinforced composite plates in thermal environments. Composite Structures 91(1): 9–19.

Shi, D.L., Feng, X.Q., Huang, Y.Y., Hwang, K.C., Gao, H. (2004). The effect of nanotube waviness and agglomeration on the elastic property of carbon nanotube reinforced composites. Journal of Engineering Materials and Technology 126(3): 250–257.

Soltanimaleki, A., Foroutan, M., Alihemmati, J. (2015). Free vibration analysis of functionally graded fiber reinforced cylindrical panels by a three dimensional mesh-free model. Journal of Vibration and Control Doi: 10.1177/1077546315570717

Yaghoobi, H., Torabi, M. (2013). Post-buckling and nonlinear free vibration analysis of geometrically imperfect functionally graded beams resting on nonlinear elastic foundation. . Applied Mathematical Modelling 37: 8324-8340.

Yas, M.H., Heshmati, M. (2012). Dynamic analysis of functionally graded nanocomposite beams reinforced by randomly oriented carbon nanotube under the action of moving load. Applied Mathematical Modeling 36(4): 1371-1394.

Yas, M.H., Samadi, N. (2012). Free vibrations and buckling analysis of carbon nanotube-reinforced composite Timoshenko beams on elastic foundation. International Journal of Pressure Vessels and Piping 98: 119-128.

Ying, J., Lü, C.F., Chen, W.Q. (2008). Two-dimensional elasticity solutions for functionally graded beams resting on elastic foundations. Composite Structures 84: 209-219.

Zhu, R., Pan, E., Roy, A.K. (2007). Molecular dynamics study of the stress–strain behavior of carbon-nanotube reinforced Epon 862 composites. Materials Science and Engineering: A 447(1-2): 51–57.